

Carderock Division, Naval Surface Warfare Center

Bethesda, Maryland 20084-5000

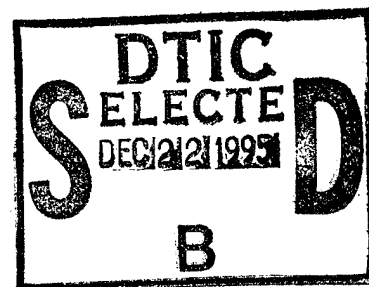
CARDIVNSWC-TR-95/122 November 1995

Hydromechanics Directorate
Research and Development Report

A Contrarotating Propeller Design for a High Speed Patrol Boat with Pod Propulsion

by
Benjamin Y.-H. Chen
Carol L. Tseng

The main text of this report was presented at the
FAST '95, Lubeck-Travemunde, Germany,
25-27 September 1995.



19951220 005

A Contrarotating Propeller Design for a High Speed
Patrol Boat with Pod Propulsion

CARDIVNSWC-TR-95/122



Approved for public release; distribution is unlimited.

UNCLASSIFIED

SECURITY CLASSIFICATION OF THIS PAGE

REPORT DOCUMENTATION PAGE

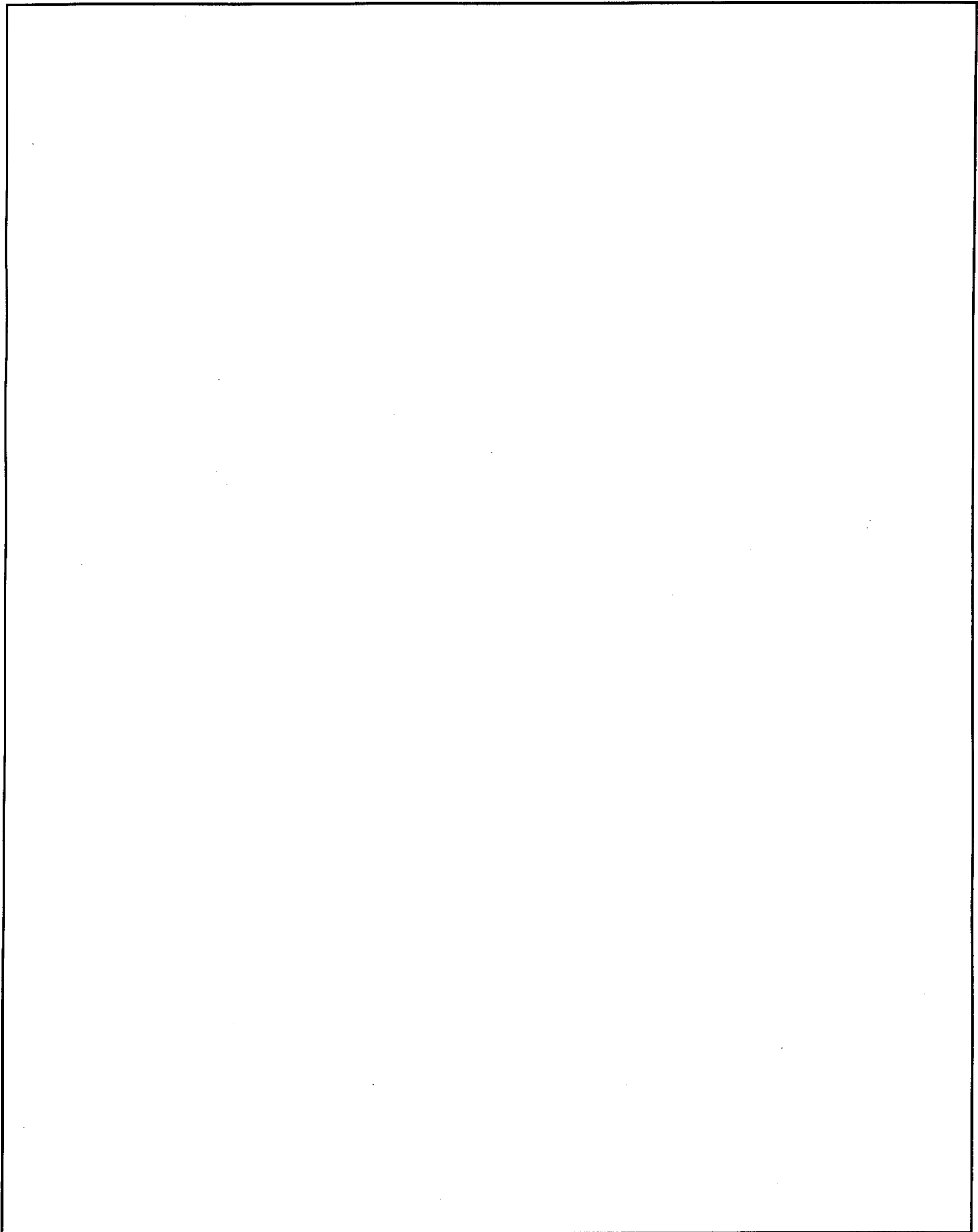
1a. REPORT SECURITY CLASSIFICATION UNCLASSIFIED		1b. RESTRICTIVE MARKINGS	
2a. SECURITY CLASSIFICATION AUTHORITY		3. DISTRIBUTION/AVAILABILITY OF REPORT Approved for public release; distribution is unlimited.	
2b. DECLASSIFICATION/DOWNGRADING SCHEDULE			
4. PERFORMING ORGANIZATION REPORT NUMBER(S) CARDIVNSWC-TR-95/122		5. MONITORING ORGANIZATION REPORT NUMBER(S)	
6a. NAME OF PERFORMING ORGANIZATION Carderock Division Naval Surface Warfare Center	6b. OFFICE SYMBOL (If applicable) Code 544	7a. NAME OF MONITORING ORGANIZATION	
6c. ADDRESS (City, State, and ZIP Code) Bethesda, MD 20084-5000		7b. ADDRESS (CITY, STATE, AND ZIP CODE)	
8a. NAME OF FUNDING/SPONSORING ORGANIZATION Advanced Surface Machinery Program	6b. OFFICE SYMBOL (If applicable) Code 808	9. PROCUREMENT INSTRUMENT IDENTIFICATION NUMBER	
8c. ADDRESS (City, State, and ZIP code) Propulsion and Auxiliary Systems Department David Taylor Model Basin Bethesda, Maryland 20084-5000		10. SOURCE OF FUNDING NUMBERS	
		PROGRAM ELEMENT NO. 63724N	PROJECT NO. WX00103
		TASK NO. R0829-802	WORK UNIT ACCESSION NO.
11. TITLE (Include Security Classification) A Contrarotating Propeller Design for a High Speed Patrol Boat with Pod Propulsion			
12. PERSONAL AUTHOR(S) Chen, Benjamin Y.-H. and Tseng, Carol L.			
13a. TYPE OF REPORT Final	13b. TIME COVERED FROM 2/89 TO 6/89	14. DATE OF REPORT (Year, Month, Day) 1995 November	15. PAGE COUNT 24
16. SUPPLEMENTARY NOTATION Main text was presented at FAST '95, Lubeck-Travemunde, Germany, 25-27 September 1995			
17. COSATI CODES		18. SUBJECT TERMS (Continue on Reverse If Necessary and Identify by Block Number)	
FIELD	GROUP	SUB-GROUP	
		Contrarotating Propeller, Pod Propulsion	
19. ABSTRACT (Continue on reverse if necessary and identify by block number) A contrarotating (CR) propeller design with a tractor pod for a high speed patrol boat is addressed. In the current arrangement, a CR propeller is placed at the forward end of a pod which is aligned with the local inflow. The powering and cavitation experiments show the performance prediction agree well with measurements. Compared to the existing controllable pitch propeller with shaft and strut configuration, the pod-mounted CR propeller show a 28% reduction in power consumption at design speed with a 7 knot improvement in cavitation inception speed. At full power, a larger pod is required, which will reduce the gain in power consumption.			
DTIC QUALITY INSPECTED 3			
(Continued on reverse side)			
20. DISTRIBUTION/AVAILABILITY OF ABSTRACT <input checked="" type="checkbox"/> UNCLASSIFIED/UNLIMITED <input type="checkbox"/> SAME AS RPT. <input type="checkbox"/> DTIC USERS		21. ABSTRACT SECURITY CLASSIFICATION UNCLASSIFIED	
22a. NAME OF RESPONSIBLE INDIVIDUAL Benjamin, Y.-H.Chen		22b. TELEPHONE (Include Area Code) (301) 227-2258	22c. OFFICE SYMBOL Code 544

DD FORM 1473, 84 MAR

UNCLASSIFIED
SECURITY CLASSIFICATION OF THIS PAGE

UNCLASSIFIED

SECURITY CLASSIFICATION OF THIS PAGE



UNCLASSIFIED

SECURITY CLASSIFICATION OF THIS PAGE

CONTENTS

	Page
Nomenclature	v
Abstract	1
Administrative Information	1
Introduction	1
Summary of Design Method	2
Design Principle	3
Design Procedure	3
Podded Contrarotating Propeller Design	6
Boat Information	6
Design Requirements	6
Wake Survey	6
Parametric Study	7
Preliminary Design	8
Intermediate Design	9
Final Design	9
Performance Predictions and Experimental Results	11
Self-Propulsion Tests	11
Cavitation Tests	14
Conclusions and Recommendations	15
Acknowledgment	15
Appendix: A. Detailed Design Information	17
References	21

FIGURES

1. An arrangement of CR propeller with tractor pod	2
2. Optimum and unloaded circulation distributions for forward and aft propellers.....	8
3. Pitch distribution for forward and aft propellers.....	10
4. Camber distribution for forward and aft propellers	10
5. Side and forward views of podded CR propellers	11

CONTENTS (CONTINUED)

	Page
6. Predicted and measured self propulsion test results.....	12
A.1. Chordlength distribution for forward and aft propellers.....	18
A.2. Thickness distribution for forward and aft propellers.....	18
A.3. Skew distribution for forward and aft propellers.....	19
A.4. Maximum blade stress distribution for forward and aft propellers.....	19

TABLES

1. Podded CR propeller design—Summary.....	7
2. Predicted and measured powering performance of podded CR propeller design represented as a unit.....	13
3. Comparisons of predicted and measured cavitation inception speeds of podded CR propeller design.....	14
A.1. Final design geometry for CR propulsor.....	20

Accession For	
NTIS GRA&I	<input checked="" type="checkbox"/>
DTIC TAB	<input type="checkbox"/>
Unannounced	<input type="checkbox"/>
Justification	
By _____	
Distribution/	
Availability Codes	
Dist	Avail and/or Special
A-1	

NOMENCLATURE

c/D	Chord to diameter ratio
D_r	Rotor diameter
EAR	Expanded area ratio
f_m/c	Maximum camber to chord length ratio
G	Nondimensional circulation
i_T/D	Total rake to diameter ratio
J_A	Advance coefficient
K_Q	Torque coefficient
K_T	Thrust coefficient
N_r	Rotor RPM
P/D	Pitch to diameter ratio
P_D	Effective horsepower
P_E	Delivered horsepower
Q	Torque
Re	Reynolds Number
t	Thrust deduction fraction
t/c	Thickness to chord ratio
T	Thrust
u_{ij}	Velocity induced by Z blades of the forward propeller
w_T	Taylor wake fraction
X_R	Nondimensional radius measured from the shaft axis
Z	Blade number
β_i	Hydrodynamic pitch angle
δ_k	Angle between adjacent blades
η_R	Relative rotative efficiency
η_o	Open water efficiency
η_D	Propulsive efficiency
θ_s	Skew angle
σ_i	Cavitation index

All other notation in this report is in accordance with the International Towing Tank Conference (ITTC)

Standard Symbols.*

* "International Towing Tank Conference Standard Symbols 1976," The British Ship Research Association, BSRA Technical Memorandum No. 500 (May 1976).

THIS PAGE INTENTIONALLY LEFT BLANK

ABSTRACT

A contrarotating (CR) propeller design with a tractor pod for a high speed patrol boat is addressed. In the current arrangement, a CR propeller is placed at the forward end of a pod which is aligned with the local inflow. The powering and cavitation experiments show the performance prediction agree well with measurements. Compared to the existing controllable pitch propeller with shaft and strut configuration, the pod-mounted CR propeller shows a 28 % reduction in power consumption at design speed with a 7 knot improvement in cavitation inception speed. At full power, a larger pod is required, which will reduce the gain in power consumption.

ADMINISTRATIVE INFORMATION

Work for this project was sponsored by the Shipboard Energy Research and Development Office of the Carderock Division, Naval Surface Warfare Center. The work was performed by the Propulsor Technology Branch (Code 544) under Program Element Number 63724N, Task Area R0829-802.

INTRODUCTION

Over the past several years, there has been a renewed interest in finding more efficient and quieter propulsors for high speed patrol boats. Conventional propulsors mounted on inclined, strut supported shafts are the typical propulsion systems found on present patrol boats. The inclined flow results in the blade angle of attack variation and thus produce early blade cavitation.

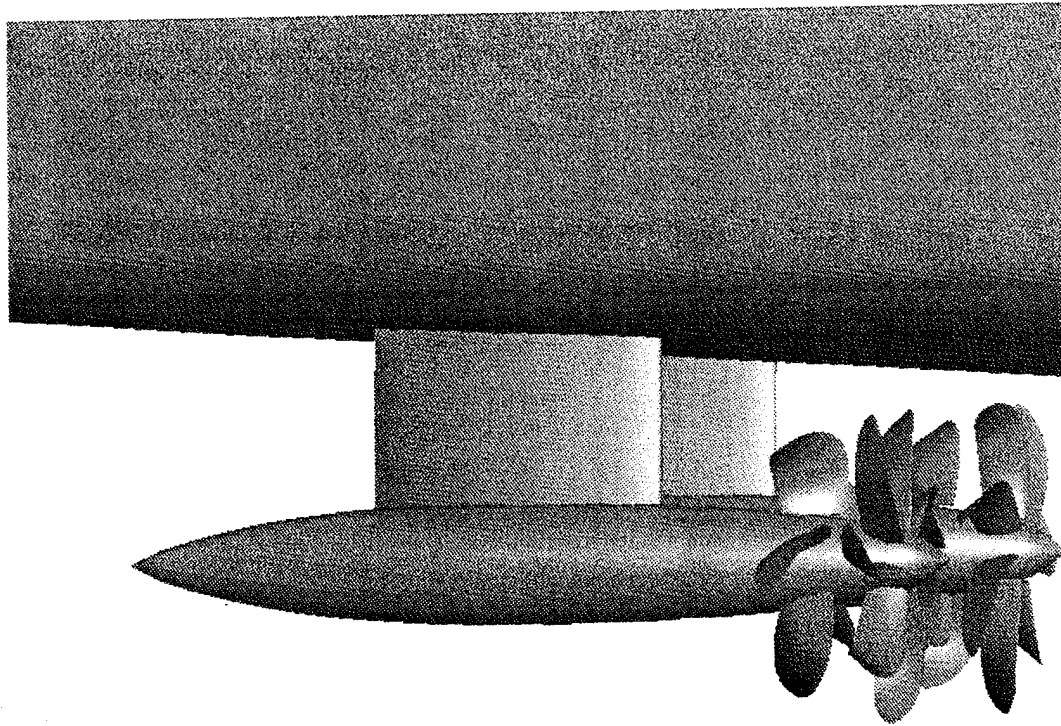


Fig. 1. An Arrangement of CR propeller with tractor pod.

In the current arrangement, contrarotating (CR) propellers are mounted at the forward end of a pod, as shown in Figure 1 and are powered by an electric motor contained within the pod. The advantages of this arrangement are that the propulsor is placed outside the hull wake and no shaft and strut is forward of the propulsor to produce nonuniformities in the inflow. Elimination of nonuniformities in the inflow results in the propeller blade sections having a nearly constant angle of attack, which greatly improves the cavitation performance. The CR propellers reduce rotational and axial kinetic energy losses in the propeller slip stream, as compared to single rotation (SR) propellers, and reduce power consumption. Additionally, in the current arrangement, the replacement of shaft and strut with the combination of pod and trim flaps also reduces power consumption at design speed. However, at full power, the benefit of power consumption gain will be reduced as a result of a larger pod to drive the propulsors.

SUMMARY OF DESIGN METHOD

The design method used for the contrarotating propellers developed by Chen and Reed¹ will be briefly summarized in the following sections. A quasi-steady cavitation prediction method was developed in this report.

DESIGN PRINCIPLE

The design method for contrarotating propellers is based on basic hydrodynamic principles of conservation of momentum, mass and circulation. To satisfy the conservation of momentum, the net force produced by the contrarotating propellers must overcome bare body drag and drag due to hull-propeller interactions. Conservation of mass is used to determine the circulation of the aft propeller once the circulation of the forward propeller is set. Conservation of circulation is used to determine the magnitude of the aft propeller circulation once the forward propeller circulation is set.

DESIGN PROCEDURE

The design procedure includes three phases: specification of operating conditions, design, and analysis.

Specification of Operating Conditions

In the first phase, the design requirements and wake survey data are provided. The effects of the hull on the flow and hull-propulsor interaction are traditionally represented by the nominal wake and two interaction coefficients: the thrust deduction factor and the wake fraction.

Design

In the design phase, there are three design stages: preliminary, intermediate, and final.

Preliminary Design. Using lifting-line theory, the preliminary design stage employs a parametric study to determine optimum forward and aft propeller diameters, rotation speed, and number of blades. In this stage, the forward and aft propeller circulation distributions are also determined. Propulsive efficiency and cavitation are considered during this stage. The lifting-line theory developed by Kerwin et al.² was employed in the current study.

Intermediate Design. In the intermediate design stage, cavitation and strength are the major factors guiding the selection of chordlength, thickness, and blade loading distribution for the forward and aft propellers. Consideration is also given to strength requirements and propulsive efficiency which are affected by these parameters. Stress calculations for the forward and aft propellers were performed using a simple beam theory (Schott et al.³).

The cavitation prediction method for the forward propeller is the same as for conventional single rotation propellers, since there is no other component ahead of it. The cavitation inception prediction method for the aft propeller developed in this report is a quasi-steady prediction method. It is composed of two steps: inflow calculations and cavitation calculations. This method is considered quasi-steady because the induced velocities from the forward propeller are held steady for one calculation of the cavitation inception on the aft propeller. Then, the forward propeller is rotated $\Delta\theta$ and another calculation of the cavitation inception on the aft propeller is performed.

The calculation of the total inflow wake starts with the calculation of the induced velocities from the forward propeller on the aft propeller using a modified version of the lifting surface program developed by Chen and Reed⁴. These calculated induced velocities, though based only on theoretical prediction, show the same trends as induced velocities measured in experiments by Jessup⁵. The velocity field of a Z-bladed propeller is obtained by shifting the induced velocities from the key blade through one blade interval and superimposing the result Z times. Thus

$$u_{ij}(\theta) = \sum_{k=1}^Z u_{ij}^*(\theta + \delta_k) \quad , \quad (1)$$

where

$$\delta_k = \frac{2\pi(k-1)}{Z} \quad k=1,2,\dots,Z \quad (2)$$

u_{ij}^* is the velocity induced by one blade and u_{ij} is the velocity induced by Z blades of the forward propeller. δ_k is the angle between adjacent blades of the forward propeller. The addition of the induced velocities to the incoming wake is the total inflow wake to the aft propeller. For contrarotating propellers an additional step is required. Since the aft propeller rotates in the opposite direction of the forward propeller, the induced velocities must undergo a mirror image transformation before its addition to the incoming wake. The mirror image was done by the following procedure:

$$\theta = 360^\circ - \theta \quad (3)$$

$$u_{ij} = -u_{ij} \quad (4)$$

The second step of the quasi-steady cavitation inception prediction method uses a two-dimensional airfoil theory developed by Brockett⁶ to compute the blade surface cavitation using the total inflow wake described earlier. To simulate the rotation of the forward component, the key blade of the forward propeller is rotated in intervals of $\Delta\theta$ and cavitation analysis is performed after each rotation. The quasi-steady method is completed when the key blade is rotated so that it passes the location of the first blade.

The tip vortex cavitation index⁷ was calculated as follows:

$$\sigma_i = K \left(\frac{G}{c/D} \right)_{0.9R}^2 (Re_{0.9R})^{0.4} \quad (5)$$

where K is an empirical coefficient determined from full scale experiments.

Final Design. The final design stage consists of using lifting-surface theory to incorporate three-dimensional effects in the design. The final pitch and camber distributions are determined using the CR lifting-surface program developed by Chen and Reed⁴. This program is a modified version of Wang's⁸ SR lifting-surface program which includes hub effects.

Analysis

In the analysis phase, steady and unsteady forces and moments are computed. The inverse lifting-surface theory developed by Greeley and Kerwin⁹ was employed.

PODDED CONTRAROTATING PROPELLER DESIGN

BOAT INFORMATION

The high speed patrol boat is a round bilge planing hull craft with a length of 154 ft (46.94 m) and displacement of 260 tons (264.2 tonnes). The existing hull has a diesel/gas turbine twin screw propulsion system. A controllable pitch propeller with shaft and strut system was mounted on each shaft.

In the current study, the shaft and strut system has been replaced by a podded system which is powered by an electrical motor contained within the pod. The pod length is 20 ft (6.10 m) with a length to diameter ratio of 7. Because of the replacement of the shaft and strut system, trim flaps and a transom extension were designed. The trim flaps decreased the boat resistance significantly, but the transom extension increased the resistance slightly. Compared to the existing shaft and strut system, the total resistance reduced substantially with a podded system at design speed.

However, the pod used in this study is not large enough to accommodate machinery to drive the propulsors at full power. A larger pod is required to house the machinery to go full power. It is expected that the increased resistance due to the larger pod will significantly reduce the gain in power consumption.

DESIGN REQUIREMENTS

The podded CR propeller was designed at the operating point for a high speed patrol boat. The boat speed was chosen at 20 knots (10.3 m/s). The thrust loading coefficient, C_{Th} , is 0.280. The forward propeller diameter is 7.56 ft (2.30 m) and rotational speed is 117 rpm. The blade numbers of the forward and aft propellers are 7 and 5, respectively. The boat's full power condition is at a shaft horsepower of 2,970 Hp (2,216 KW) per pod (twin pods) and a rotational speed of 174 rpm.

WAKE SURVEY

The resistance and stock powering tests and wake survey were performed at the David Taylor Model Basin (DTMB) towing tank. At the design boat speed of 20 knots, the effective horsepower is 1,550 hp. The thrust deduction and wake fraction are 0.885 and 1.0, respectively from the model propulsion test.

PARAMETRIC STUDY

The design parameters for the present study were chosen based on a parametric study. The aft propeller diameter was determined through mass conservation and showed an optimum diameter of 95 % of the forward propeller diameter. In order to make certain that the tip vortex of the forward propeller does not impinge upon the aft propeller, the final aft propeller diameter, which is 85 % of the forward propeller diameter, was chosen to be slightly smaller than the preliminary diameter computed using mass conservation. The axial spacing between the proximate propellers was chosen to be one quarter of the forward propeller diameter. A summary of the design parameters for the podded CR propeller is given in Table 1.

Table 1. Podded CR propeller design—Summary.

	Forward Propeller	Aft Propeller
Boat Speed (knots)	20	20
Rotational Speed (rpm)	117	117
Thrust Loading Coefficient	0.2800	
Geometry		
Diameter (ft)	7.56	6.43
Number of blades	7	5
Expanded Area Ratio	0.501	0.563
Skew (deg)	25	25
Total Rake	0	0
Blade Sections	*	*
Axial Spacing (ft)	1.89	
* NACA 66 (TMB Modified) Thickness, NACA a = 0.8 Meanline		

PRELIMINARY DESIGN

The preliminary design consists of lifting-line calculations. The optimum circulation distributions and the unloaded circulation distributions for the forward and aft propellers are shown in Figure 2. For both the forward and aft propellers, the hub and the tip were unloaded; the loading was shifted inboard. The advantages of unloading the blade root and tip are to help delay blade hub and tip vortex cavitation inception and to reduce the tendency toward cavitation erosion near the blade root and tip.

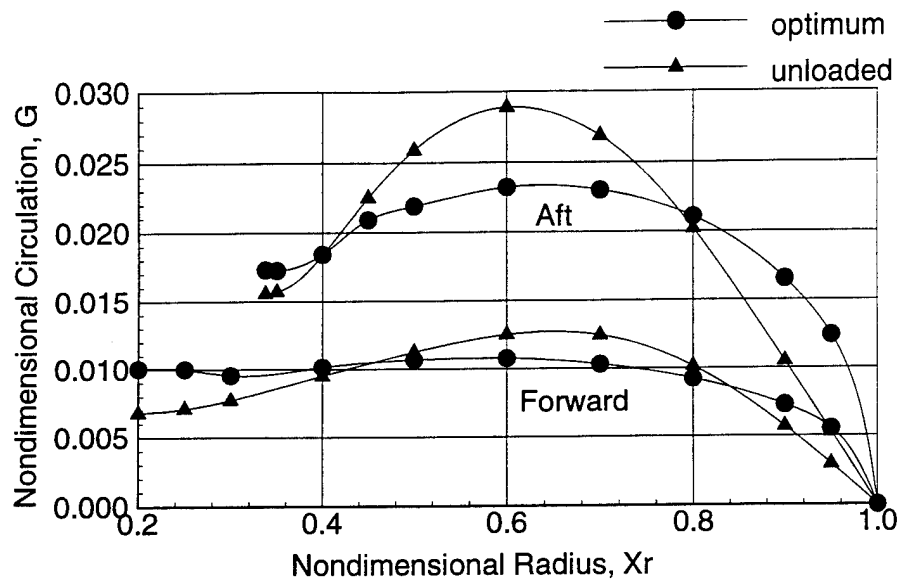


Fig. 2. Optimum and unloaded circulation distributions for forward and aft propellers.

The following guidelines for unloading the hub were employed: (1) The net circulation at the root is zero to minimize the hub vortex strength; (2) The slope of the circulation at the root is almost zero to minimize the trailing edge vortex sheet. The circulation distribution was constrained to keep the lift coefficient below 0.5. This constraint limited the amount of unloading at the tip since the increased loading inboard brought the lift coefficient to the 0.5 limit. The same guidelines were used in determining the circulation distributions of both propellers. Due to these constraints, there was a 5% loss in efficiency between the optimum and unloaded cases.

The thickness and chordlength distributions, shown in the Appendix, were determined from the strength analysis and cavitation performance predictions. When the final thickness and chordlength distributions were determined during the intermediate design phase, the lifting-line calculations were redone with the new geometry.

Based on the unsteady force calculation, a skew distribution, shown in the Appendix, was chosen for the forward and aft propellers to minimize unsteady forces. A nonlinear skew distribution with 25 degrees tip skew was selected. Zero total rake was used in this design.

INTERMEDIATE DESIGN

The intermediate design phase includes strength analysis and cavitation performance predictions. The strength requirement for the propellers was 12,500 psi maximum stress for nickel aluminum bronze material at the full power condition. The stress distribution is shown in the Appendix.

The blade surface cavitation analysis of the forward propeller was straightforward since the inflow wake was nearly uniform and there were no components in front of the forward propeller. The cavitation analysis for the aft propeller was significantly more complicated because of the effect of the forward propeller wake on the aft propeller. The quasi-steady analysis method described previously was used for the aft propeller.

The calculation for tip vortex cavitation was specified in Eq. 5. Hub vortex cavitation prevention was also addressed in the preliminary design phase. The circulations at the roots of the forward and after propeller blades were chosen to be equal in magnitude and opposite in direction so that the net circulation from both propellers was zero. This procedure attempts to minimize the hub vortex strength. Also, the spanwise gradient of circulation at the root was chosen to be essentially zero for each propeller to inhibit trailing vortex sheet formation.

FINAL DESIGN

The final design phase includes the lifting-surface design calculations. Both forward and aft propellers had a NACA $a = 0.80$ meanline chordwise loading distribution from cavitation and viscous flow points of view. A modified NACA 66 thickness distribution was selected for the present application. Figures 3 and 4 show the respective final pitch and camber distributions for the forward and aft propellers. A solid model rendering of the podded CR propellers is generated on a CAD system and is shown in Figure 5. The final geometry specifications are shown in the Appendix.

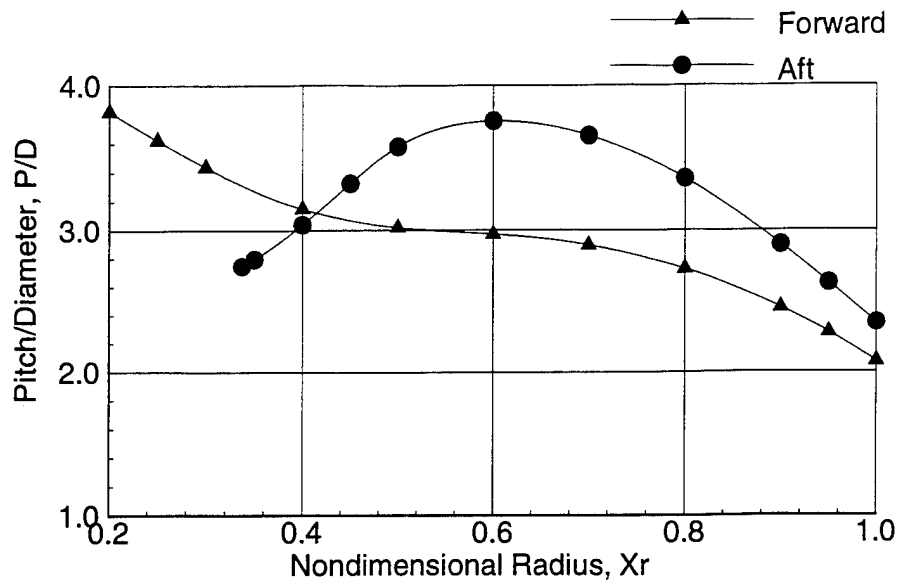


Fig. 3. Pitch distribution for forward and aft propellers.

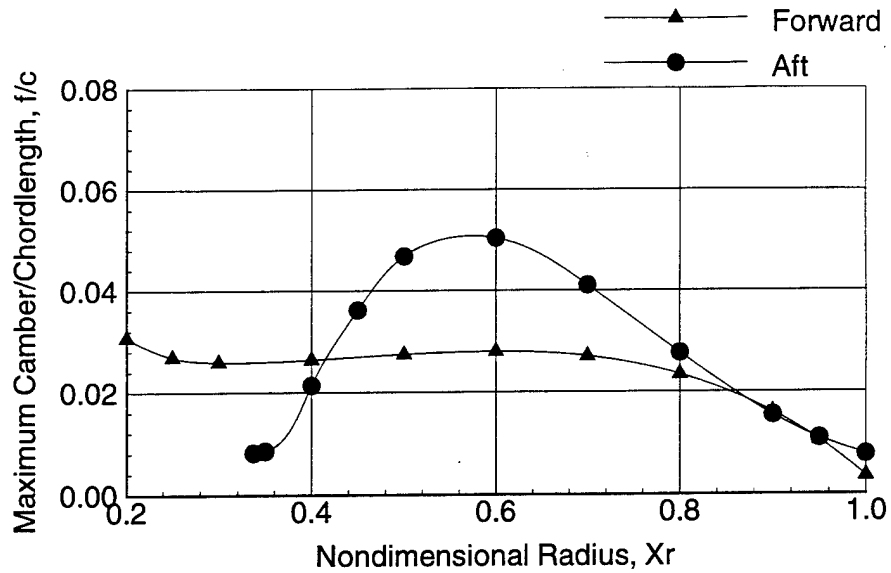


Fig. 4. Camber distribution for forward and aft propellers.

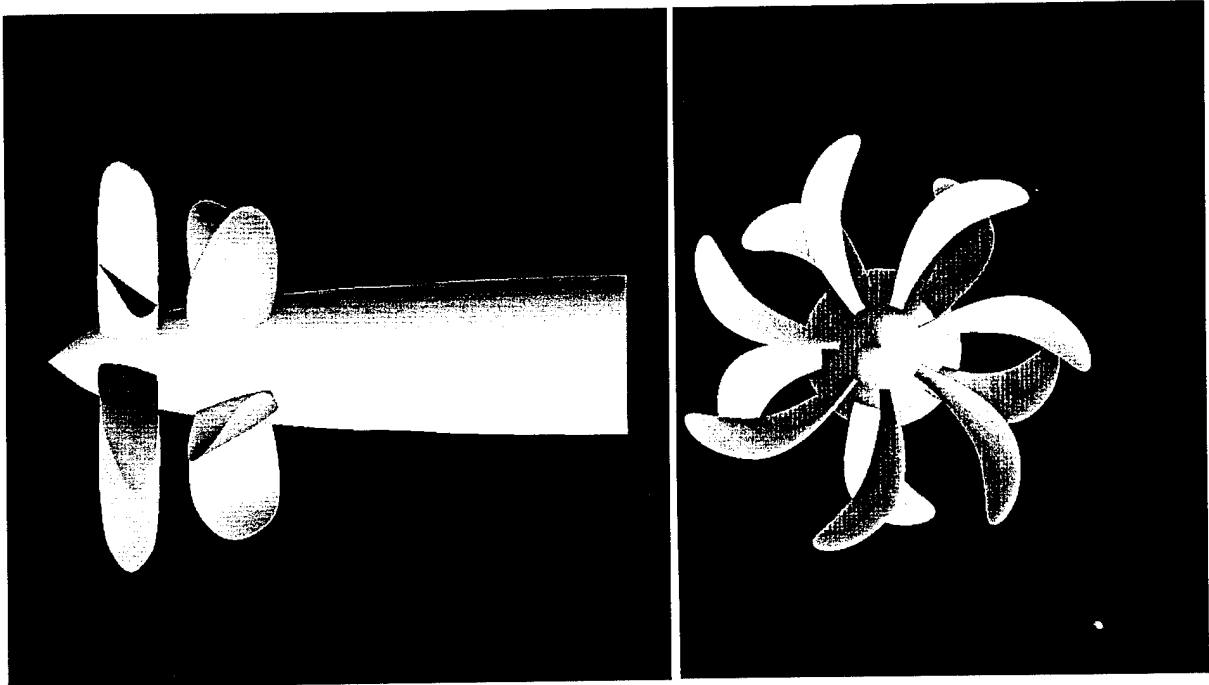


Fig. 5. Side and forward views of podded CR propellers.

PERFORMANCE PREDICTIONS AND EXPERIMENTAL RESULTS

Aluminum models of the forward and aft propellers were manufactured based on the final design geometry. The model propellers 5112 and 5114 represent the forward propellers and 5113 and 5115 represent aft propellers.

SELF-PROPULSION TESTS

Self-propulsion tests were conducted in the David Taylor Model Basin (DTMB) towing tank. The boat model 5365-A used for the resistance and self-propulsion tests of the podded CR propellers had previously been used for the resistance and self-propulsion tests of the SR propeller. Figure 6(a) shows the measured delivered power as a function of boat speed and compares the predicted value with the measured. Figure 6(b) shows the measured rotational speed as a function of boat speed and compares the predicted value with the measured. The predicted and measured self-propulsion performance at the design boat speed of the podded CR propeller is shown in Table 2.

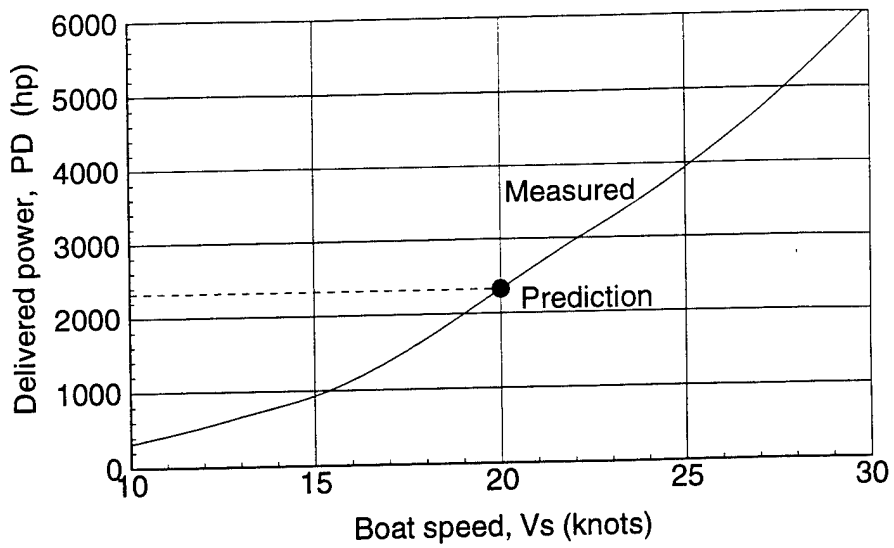


Fig. 6a. Delivered Power.

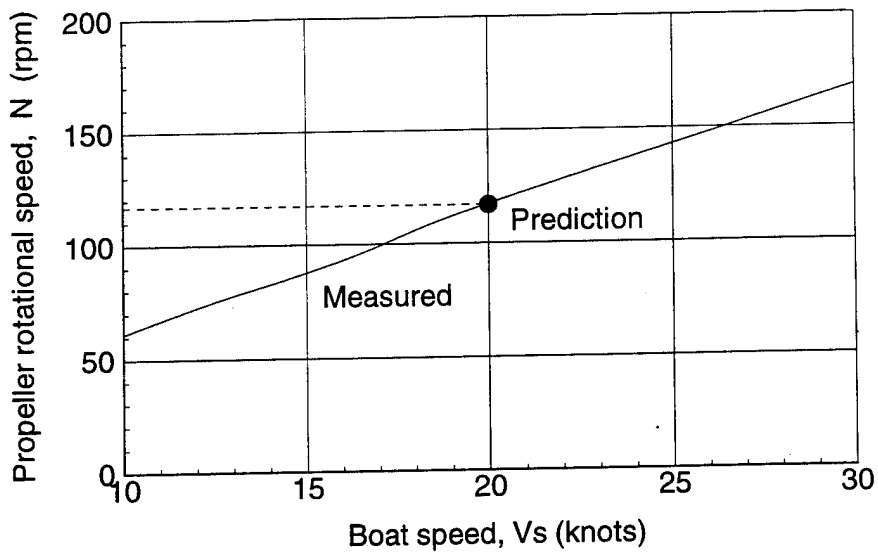


Fig. 6b. Rotation speed.

Fig. 6. Predicted and measured self propulsion test results.

Table 2. Predicted and measured powering performance of podded CR propeller design represented as a unit.

	Design	Self-propulsion Experiment
V_s (knots)	20	20
PE (hp)	1,550 (-4.3%)	1,620
PD (hp)	2,323 (0.1%)	2,320
1-t	0.885 (-2.7%)	0.910
1-wT	1.000 (-2.0%)	1.020
JA	2.290 (-1.5%)	2.325
N (rpm)	117(-0.3%)	117.4
KT	0.580 (-0.3%)	0.582
KQ	0.279(1.0%)	0.276
η_R	1.010 (2.0%)	0.990
η_O	0.756(-4.9%)	0.795
η_D	0.670 (-4.3%)	0.700

The effective horsepower (EHP) used in the design is 4.3% lower than the measurement. Modifications made to the test boat most likely account for the higher experimental EHP. The predicted delivered power is almost identical to the measured value. The estimated thrust deduction and wake fraction for the design are 2.7% and 2.0% lower than the measurement. Therefore, the actual drag due to the presence of the propeller was lower than the drag used in the design. This miscalculation probably resulted in lessening the difference between the measured and estimated EHP.

The design advance coefficient is 1.5 % lower than the measurement, and the predicted rotation speed is almost equivalent to the measurement. The predicted thrust is almost identical, and the predicted torque is 1.0 % higher than the measurement. The predicted relative rotative efficiency is 2.0 % higher than the measurement. The predicted open water efficiency and propulsive efficiency are 4.9% and 4.3 % lower than the measurement. These discrepancies primarily result from the difference between the design and the measured effective horsepower. In general, the accuracy of the experimental measurements with the CR propeller is $\pm 2\%$ on thrust and torque. Overall the predicted values agree well with the experimental measurements, and in general are within the accepted accuracy of the experimental measurements.

CAVITATION TESTS

Cavitation tests were performed at the Applied Research Laboratory/Pennsylvania State University (ARL/PSU) 48 inch water tunnel. Table 3 shows the cavitation inception speed difference between the design and the measured values (designed value - measured value). There were no predicted leading edge suction side (LESS), leading edge pressure side (LEPS), pressure side back bubble (PSBB), and pressure side tip vortex (PSTV) cavitation for the forward and aft propellers as the measurements showed. The predicted suction side back bubble (SSBB) cavitation for the forward and aft propellers were 3 knots and 1 knot higher than the measurement. Calculated suction side tip vortex (SSTV) for the aft propeller came in 2 knots higher than the measurement, and there was no predicted and measured SSTV for the forward propeller. The good agreement between the experimental data and the predicted cavitation inception speeds gives us confidence in the quasi-steady cavitation prediction method developed for this design.

Table 3. Comparisons of predicted and measured cavitation inception speeds of podded CR propeller design.

	Forward propeller	Aft Propeller
SSBB (knots)	3	1
SSTV (knots)	--	2

Note: Inception speed comparisons are
designed value-measured value
SSBB - suction side back bubble cavitation
SSTV - suction side tip vortex cavitation

CONCLUSIONS AND RECOMMENDATIONS

The following conclusions can be drawn from the present study.

- Self-propulsion and cavitation experiments show that the performance predictions agree well with the experimental measurements.
- The pod-mounted CR propeller design achieves the design goals of reducing power consumption and increasing cavitation inception speed with no degradation in overall performance. Compared to the existing controllable pitch propeller with shaft and strut configuration, the pod-mounted CR propeller shows a 28 % reduction in power consumption with a 7 knot improvement in cavitation inception speed. Rotational energy recovery of the CR propeller results in energy saving of 10 %. The larger CR propeller diameter contributes an additional 4 % energy saving over the SR propeller. At design speed, the combined effect of pod and trim flaps results in 14 % energy saving due to removing shaft and strut. However, a larger pod is needed to obtain full power and will reduce the improvement in energy saving.

A steering pod which can be adjusted with the inflow direction was not considered in the current study but has been recommended for future work. This arrangement improves cavitation performance during maneuvering.

ACKNOWLEDGMENT

The authors would like to thank Mr. Ken Remmers and Mr. Bill Cave of DTMB for carrying out the open-water and self-propulsion experiments. The authors would also like to thank Mr. J. Oefelein of ARL/PSU for conducting the cavitation measurements.

THIS PAGE INTENTIONALLY LEFT BLANK

APPENDIX A

DETAILED DESIGN INFORMATION

This section provides additional information for the original report. Based on cavitation, flow separation, and efficiency considerations, the chord-length distributions of the forward and aft propellers were chosen. The chord distributions for the forward and aft propellers are shown in Figure A.1.

The thickness distribution was selected based on strength and cavitation considerations. Figure A.2 shows the thickness distributions for the forward and aft propellers.

As shown in Figure A.3, a tip skew distribution of 25 degrees, varying nonlinearly from zero at the hub, was selected for the forward and aft propellers. The total rake for both forward and aft propellers was zero. Therefore, they have negative rake to offset the skew-induced rake. The stress distributions computed by beam theory corresponding to these choices of geometry are given in Figure A.4.

The final geometric specifications of the podded CR propulsor, including the details of the leading and trailing edges, were computed using the computer code, XYZ-PROP, developed by Brockett¹⁰. All the input data: chord length, thickness, skew, pitch, and camber distributions were faired by a cubic spline procedure before being input to XYZ-PROP. A list of the chord length, thickness, skew, pitch and camber distributions are given in Table A.1.

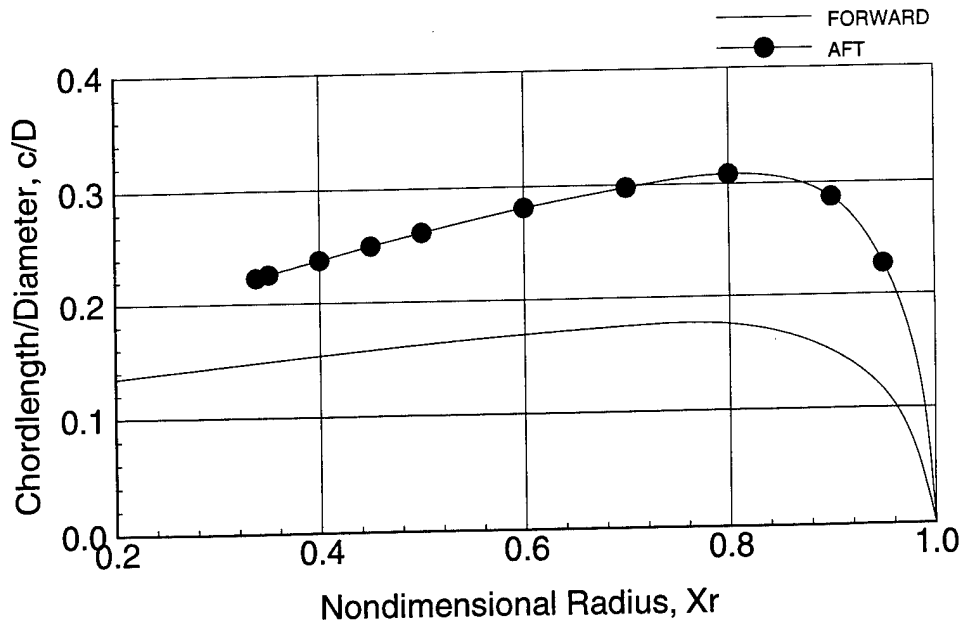


Fig. A.1. Chordlength distribution for forward and aft propellers.

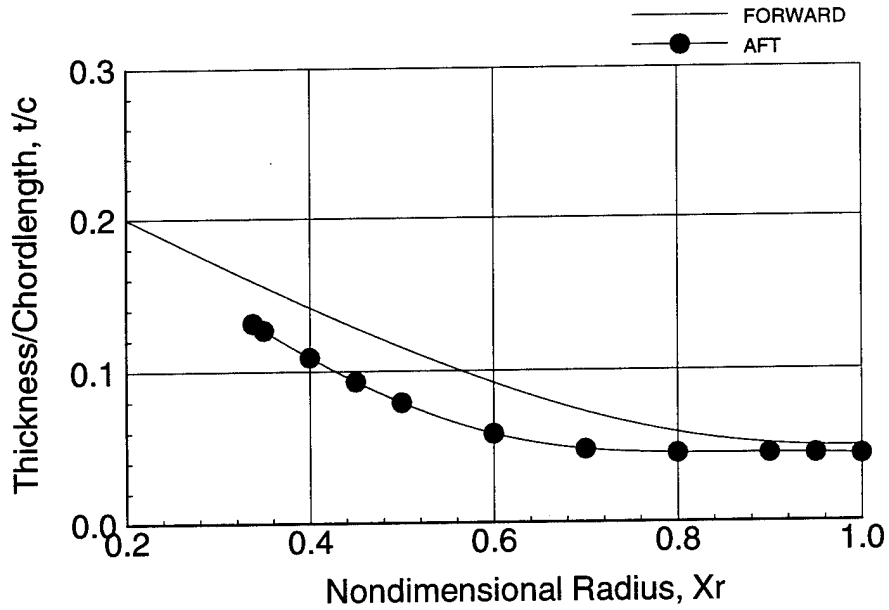


Fig. A.2. Thickness distribution for forward and aft propellers.

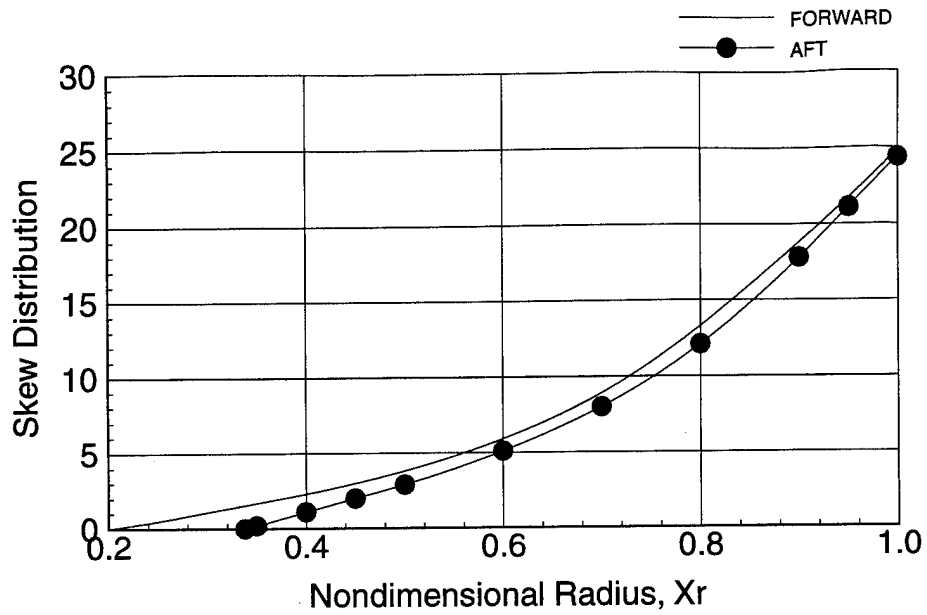


Fig. A.3. Skew distribution for forward and aft propellers.

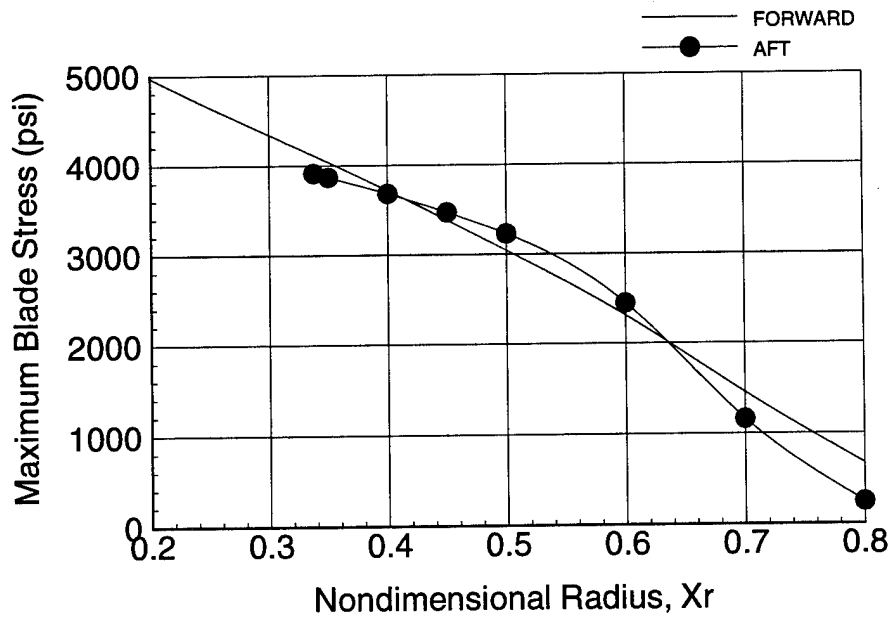


Fig. A.4. Maximum blade stress distribution for forward and aft propellers.

Table A.1. Final design geometry for CR propulsor.

Table A.1a. Forward propeller.

r/R	c/D	P/D	i_T/D	θ_s	t/c	f_m/c
0.140	0.1296	4.064	0.0	-0.6	0.2182	0.03764
0.200	0.1350	3.820	0.0	0.0	0.2000	0.03070
0.250	0.1396	3.623	0.0	0.5	0.1849	0.02690
0.300	0.1442	3.438	0.0	1.1	0.1700	0.02595
0.400	0.1533	3.150	0.0	2.3	0.1417	0.02640
0.500	0.1619	3.019	0.0	3.8	0.1155	0.02745
0.600	0.1692	2.971	0.0	5.9	0.0921	0.02795
0.700	0.1749	2.895	0.0	8.9	0.0727	0.02705
0.800	0.1754	2.727	0.0	13.3	0.0590	0.02340
0.900	0.1499	2.455	0.0	18.8	0.0514	0.01600
0.950	0.1152	2.279	0.0	21.7	0.0498	0.01050
1.000	0.0000	2.074	0.0	24.8	0.0497	0.00350

Table A.1b. Aft propeller.

r/R	c/D	P/D	i_T/D	θ_s	t/c	f_m/c
0.338	0.2230	2.750	0.0	0.0	0.1317	0.00821
0.350	0.2260	2.800	0.0	0.2	0.1270	0.00860
0.400	0.2380	3.040	0.0	1.1	0.1091	0.02138
0.450	0.2500	3.325	0.0	2.0	0.0932	0.03618
0.500	0.2613	3.581	0.0	2.9	0.0793	0.04682
0.600	0.2813	3.755	0.0	5.1	0.0587	0.05038
0.700	0.2976	3.655	0.0	8.0	0.0482	0.04103
0.800	0.3082	3.360	0.0	12.1	0.0453	0.02767
0.900	0.2872	2.899	0.0	17.8	0.0450	0.01545
0.950	0.2274	2.630	0.0	21.1	0.0448	0.01092
1.000	0.0000	2.350	0.0	24.4	0.0440	0.00776

REFERENCES

1. Chen, B. Y.-H. and A. M. Reed, "A Design Method and an Application For Contrarotating Propellers," in: Proceedings of the *22nd American Towing Tank Conference*, St. John's, Newfoundland, pp. 356-362 (1989).
2. Kerwin, J. E., W. B. Conney, and C.-Y. Hsin, "Optimum Circulation Distributions For Single and Multiple-Component Propulsors," in: Proceedings of the *21st American Towing Tank Conference*, pp. 53-60 (1986).
3. Schott, C. G., J. McMahon, P. Hargrove, and N. Hubbard, "A Computer Code for the Prediction of Propeller Blade Stress by Cantilever Beam Theory," DTRC/SHD-1151-23 (1989).
4. Chen, B. Y.-H., and A. M. Reed, "A Lifting-Surface Program For Contrarotating Propellers," in: Proceedings of the *Symposium on Hydrodynamic Performance Enhancement for Marine Applications*, Newport, RI, pp. 57-68 (1988).
5. Jessup, S. D., *An Experimental Investigation of Viscous Aspects of Propeller Blade Flow*, Ph. D. dissertation, School of Engineering and Architecture, The Catholic University of America (1988).
6. Brockett, T., "Minimum Pressure Envelopes for Modified NACA 66 Sections With NACA $a = 0.8$ Camber and BUSHIPS Type I and II Sections," David Taylor Model Basin Report 1780 (1966).
7. McCormick, B.W., Jr., "On Cavitation Produced by a Vortex Trailing from a Lifting Surface," *J. Basic Engineering*, Vol. 84, pp. 369-79 (1962).
8. Wang, M.H., "Hub Effects in Propeller Design and Analysis," Department of Ocean Engineering, MIT Report 85-14 (1985).
9. Greely, D.S. and J.E. Kerwin, "Numerical Methods for Propeller Design and Analysis in Steady Flow," *SNAME Transactions*, Vol. 90, pp. 415-453 (1982).
10. Brockett, T.E., "Analytical Specification of Propeller Blade-Surface Geometry," DTRC Ship Hydrodynamics Department Report, DTRC/SHD-699-01(1976).

THIS PAGE INTENTIONALLY LEFT BLANK

INITIAL DISTRIBUTION

Copies	Code Name	Copies	Code Name
2	CNO	1	DOT Lib
	1 N87T		
	1 N87T2	1	U. Cal. Berkley/Lib
2	ONR	1	CIT/AERO Lib
	1 344 R. Vogelsong		
	1 344 P. Majumdar	1	U. Iowa/Lib
1	ONR Boston	1	U. Michigan/Lib
1	ONR Chicago	2	MIT
		1	Barker Engr Lib
1	ONR London, England	1	Ocean Engr/ J. Kerwin
1	NRL	3	State U. Maritime Col
		1	ARL Lib
1	USNA/Lib	1	Engr Dept
		1	Inst Math Sci
1	NAVPGSCOL/Lib	3	Penn State U. APL
1	NROTC & NAVADMINU, MIT	1	Lib
		1	M. Billet
1	NADC	1	D. Thompson
1	NCCOSC RDT&E Div. T. Mautner	1	Boeing Adv Amr Sys Div
		1	Brewer Engr Lab
6	NAVSEA	1	Stanford Res Inst Lib
	1 03D		
	1 03T	1	SIT Davidson Lab/Lib
	1 03H32		
	1 03X1	1	Texas U. ARL Lib
	1 03X7		
	1 03Z	1	VPI/Dept Aero & Ocean Engr/Schetz
2	MMA	1	Webb Inst/ J. Hadler
	1 Lib		
	1 Maritime Res Ctr		
2	DTIC	1	WHOI Ocean Engr Dept
1	LC/SCI & Tech Div	1	WPI Alden Hydr Lab Lib
2	NASA STIF	1	ASME/Res Comm Info
	1 Dir Res		
1	Lib	1	ASNE
1	NSF Engr Div/Lib		

INITIAL DISTRIBUTION

Copies Code Name		DIVISION DISTRIBUTION			
Copies	Code	Name	Copies	Code	Name
1		SNAME/Tech Lib			
1		Allis Chalmers, York, PA	2	0023	Reports Control
1		AVCO Lycoming	1	011	J. Corrado
1		Baker Manufacturing	1	0114	K.-H. Kim
2		Bird-Johnson Co	1	3021	Publications
1		J. Norton	1	3023	TIC (C)
1		G. Platzer			
			1	50	W. Morgan
1		Douglas Aircraft/Lib	1	506	D. Walden
			1	508	R. Boswell
2		Exxon Res Div	1	52	W.-C. Lin
1		Lib	1	521	W. Day
1		Fitzgerald	1	522	K. Remmers
			1	54	B. Webster
1		Friede & Goldman/Michel	1	542	T. Huang
			20	544	B. Chen
1		Gibbs & Cox/Lib	1	544	C. Tseng
			1	56	D. Cieslowski
1		Rosenblatt & Son/Lib			
			1	60	G. Wacker
1		Inst for Defense Anal	1	65	R. Rockwell
1		Itek Vidya	1	70	M. Sevik
			1	7051	W. Blake
1		Lips Duran/Kress	1	7250	R. Szwerc
			1	808	C. Krolick
1		Littleton R & Engr Corp/Reed	1	808	K. Tavener
			1	821	G. Duvall
1		Litton Industries			
1		Lockeed, Palmdale/ A. Solomin			
1		Maritech, Inc./Vassilopoulos			
1		HRA/JJMA, Inc./ B. Cox			
1		AME/ O. Scherer			
1		Arete Associates/ T. Brockett			
1		Nielson Engr/Spangler			

